CRYSTALLIZATION OF MEMBRANE PROTEINS

Acta Cryst. (1994). D**50**, 632–638

In situ Two-Dimensional Crystallization of a Polytopic Membrane Protein: the Cardiac Gap Junction Channel*

BY MARK YEAGER

Departments of Cell Biology and Molecular Biology, The Scripps Research Institute, and Division of Cardiovascular Diseases, Scripps Clinic and Research Foundation, La Jolla, California 92037, *USA*

(*Received* 3 *December* 1993; *accepted* 20 *December* 1993)

Abstract

In situ crystallization of rat ventricular gap junctions was accomplished by sequential dialysis of membranes against low concentrations of deoxycholate and dodecyl-β-D-maltoside. Lipids are removed without solubilizing the protein, and the increased protein concentration in the membrane plane facilitates two-dimensional crystallization in the native membrane environment. The two-dimensional crystals have a nominal resolution of 16 Å and display plane group symmetry $p6$ with $a = b = 85$ Å and $\gamma = 120°$. Electron crystallography reveals that the cardiac gap junction membrane channel is formed by a hexameric cluster of protein subunits, and this hexameric design appears to be a recurring quaternary motif for the multigene family of gap junction proteins. Exposure of membranes to low concentrations of detergents may provide an approach for *in situ* two-dimensional crystallization of other connexins as well as other membrane proteins, especially those that are labile when solubilized as protein–detergent micelles.

Introduction

Gap junctions are specialized regions of the plasma membrane in which protein oligomers are in register between adjacent cells, thereby forming a conduit for intercellular communication that allows exchange of nutrients, metabolites, ions and small molecules up to ~1000 Da (Loewenstein, 1981). Cardiac gap junctions mediate intercellular propagation of current flow between myocytes and coordinate the synchronized contraction of the heart (Barr, Dewey & Berger, 1965).

The integral membrane proteins that form gap junctions, termed connexins, are derived from a multigene family. At least ten separate gene products have now been identified (reviewed in Beyer, Paul & Goodenough, 1990; Willecke, Hennemann, Dahl, Jungbluth & Heynkes, 1991; Kumar & Gilula, 1992). The connexins have been classified into two types, α and β, based on characteristic features of their amino-acid sequences (Kumar & Gilula, 1992). The α_1 heart connexin ($M_r = 43$ kDa) is substantially larger than the liver connexins (β_1Cx, $M_r = 32$ kDa and β_2Cx, $M_r = 26$ kDa), primarily due to a larger carboxy-terminal domain (Manjunath, Goings & Page, 1985; Manjunath, Nicholson, Teplow, Hood, Page & Revel, 1987). The amino-acid sequence of α_1Cx has been determined by molecular cloning techniques (Beyer, Paul & Goodenough, 1987), and we and others (Beyer, Kistler, Paul & Goodenough, 1989; Yancey, John, Lal, Austin & Revel, 1989; Laird & Revel, 1990; Yeager & Gilula, 1992) have determined the topology of the polypeptide using accessibility for labeling by site-specific peptide antibodies and protease cleavage. These data support a model in which α_1Cx is a polytopic membrane protein having four transmembrane domains (Fig. 1).

The inability to grow three-dimensional crystals has precluded the high-resolution structure analysis of any gap junction protein. However, gap junctions in liver plasma membranes display inherent two-dimensional crystallinity (Sikerwar & Unwin, 1988) which has made liver junctions amenable to low-resolution structure analysis using electron crystallography (Unwin & Zampighi, 1980; Unwin & Ennis, 1984; Baker, Sosinsky, Casper, Gall & Goodenough, 1985) and X-ray scattering (Caspar, Goodenough, Makowski & Phillips, 1977; Makowski, Caspar, Phillips & Goodenough, 1977). These studies provide compelling evidence that the channels in liver gap junctions are formed by a hexameric arrangement of β connexin subunits, termed a connexon.

The lack of two-dimensional crystallinity in cardiac gap junctions has impeded their structure analysis and hindered the comparison of conserved and divergent features between α and β connexins.

* Abbreviations used in this paper: Cx, connexin; α_1 = Cx43, $M_r = 43$ kDa rat cardiac gap junction protein; $\alpha_3 = 70$ kDa lens gap junction protein; β_1 = Cx32, $M_r = 32$ kDa rat liver gap junction protein; β_2 = Cx26, $M_r = 26$ kDa mouse liver gap junction protein; TBS, Tris-buffered saline; PTA, phosphotungstic acid.

ISSN 0907-4449

In this report an approach is presented for *in situ* two-dimensional crystallization of cardiac gap junctions using sequential detergent dialysis. The term *in situ* crystallization is used since the protein is examined in its native membrane environment. Mild detergent treatment removes lipids to concentrate the protein in the membrane plane and thereby facilitate crystallization. This method of *in situ* crystallization can be contrasted with two-dimensional crystallization by *in vitro* reconstitution in which the protein is solubilized in detergent, the purified protein–detergent micelles are reconstituted with lipids, and the detergent is removed by dialysis (reviewed by Kühlbrandt, 1992; Jap, Zulauf, Scheybani, Hefti, Baumeister, Aebi & Engel, 1992).

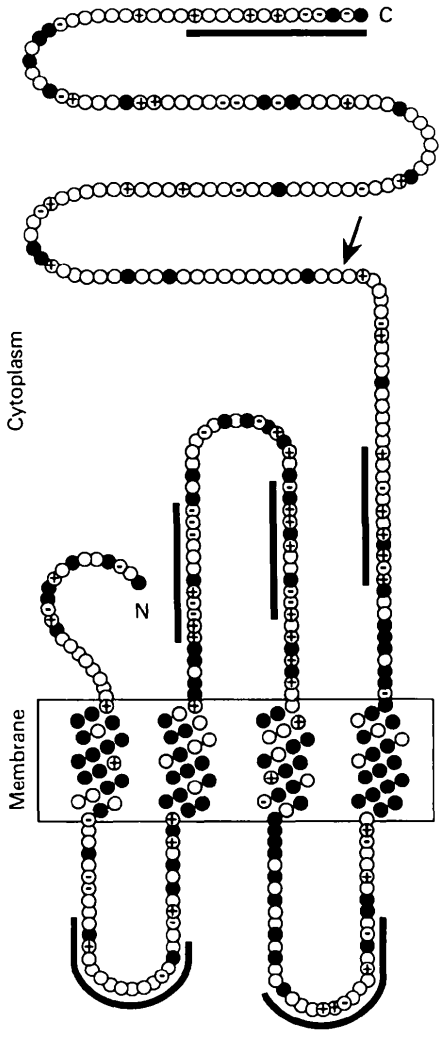

Fig. 1. The cardiac gap junction protein is a polytopic membrane protein with four membrane-spanning domains. This folding model for M_r = 43 kDa α_1 connexin (also termed connexin 43) from rat heart is supported by experiments using immunolabeling by site-specific peptide antibodies (bars) and protease cleavage (arrow) (Yeager & Gilula, 1992), and is consistent with similar work by others (Beyer, Kistler, Paul & Goodenough, 1989; Yancey, John, Lal, Austin & Revel, 1989; Laird & Revel, 1990). The locations of the cytoplasmic and extracellular regions are indicated, and the amino acids are coded as follows: solid = hydrophobic; + = basic; − = acidic. Note the clustering of hydrophobic residues in the membrane interior and the charged domains primarily at the cytoplasmic membrane surface and the carboxy tail.

Materials and methods

Isolation of cardiac gap junctions

Rat ventricular gap junctions were isolated using a method similar to that of Manjunath & Page (1986). Buffer volumes were scaled to accommodate 20 instead of four hearts, and tissue (two hearts in 20 ml buffer) was homogenized for 1 min using a Tekmar tissuemizer (Cincinnati, OH) at full power. Phenylmethylsulfonyl fluoride at a concentration of 1 m*M* was added to the isolation buffer to prevent proteolysis (Manjunath, Goings & Page, 1985). The pH of the bicarbonate buffer was maintained at ~8 by addition of 0.1 *M* NaOH. Step gradients using ultrapure sucrose (Schwarz/Mann Biotech, Cleveland, OH) allowed separation of the heavier gap junctions which floated on 49%(*w*/*v*) sucrose from the lighter mitochondrial, sarcoplasmic reticulum and sarcolemmal membranes, which floated on 35% sucrose. Contaminating collagen and other intercellular matrix proteins were pelleted during these centrifugations. Collagen contamination was minimized by using a 49% sucrose cushion in the second sucrose step gradient. The aggregation of junctional plaques was also reduced by not pelleting the junctions but simply retrieving them from the 35/49% sucrose interface of the second sucrose gradient.

SDS polyacrylamide gel electrophoresis and immunoblot analysis

Aliquots of gap junctions were solubilized at room temperature for ~20 min and analyzed using a discontinuous buffer system (Hoefer Scientific Instruments, San Francisco, CA) with 4.5% stacking gels and 11.5% separating gels (Laemmli, 1970) using Protogel bisacrylamide (National Diagnostics, Manville, NJ). Molecular weight protein standards were from Sigma Chemical Co. (St Louis, MO).

Proteins were transferred from polyacrylamide gels onto nitrocellulose (Schleicher & Schuell, Keene, NH) using an electro-transfer apparatus (Bio-Rad Chemicals, Richmond, CA) for 2 h at 55 mV (Towbin, Staehelin & Gordon, 1979). The nitrocellulose blots were blocked for at least 1 h with 3% bovine serum albumin (Boehringer Mannheim Biochemicals, Indianapolis, IN) in Tris-buffered saline (TBS = 50 m*M* Tris; 300 m*M* NaCl; pH 7.5). The

blot was then exposed for ~3 h with affinity purified antibodies directed against amino acids 131–142 in α_1Cx (Yeager & Gilula, 1992). After three ~20 min TBS washes, the blot was incubated for ~1 h with ^{125}I protein *A* at a dilution of 1:2000 (Amersham Corporation, Arlington Heights, IL) and subsequently washed with TBS as before. Autoradiography was performed using Kodak XAR-5 film at 203 K with an intensifying screen.

Two-dimensional crystallization

Cardiac gap junctions suspended in ~0.5 ml of 5.0 m*M* Trizma base (Sigma) (pH 10) containing 0.3% sodium deoxycholate (Sigma) were sonicated for 30 s at setting 4 using a Kontes micro-ultrasonicator (Vineland, NJ). The suspension was first dialyzed using Spectra/Por tubing (Spectrum Medical Industries, Inc., Los Angeles, CA) at 278 K for 24 h against 1.0 l of buffer containing 0.5%(*w*/*v*) sodium deoxycholate (Sigma), 5.0 m*M* Hepes (Sigma) (pH 8), 0.1 m*M* $CaCl_2$ (Baker), and 0.02% sodium azide (Sigma) and then for 24 h against deoxycholate-free buffer. The suspension was then dialyzed for 24 h against 0.05%(*w*/*v*) dodecyl-β-D-maltoside (CalBiochem, La Jolla, CA) with the same ingredients as the deoxycholate-free buffer plus 0.5 m*M* $MgCl_2$ (Baker). The suspension was finally dialyzed for 24–48 h against dodecylmaltoside-free buffer. The membrane crystals were stored in the final dialysis buffer at 278 K and were stable for at least a month.

Electron microscopy

Aliquots of gap junctions were deposited on acetone-washed, carbon-coated, glow-discharged, 400 mesh copper grids (Ernest F. Fullam, Inc., Latham, NY) by centrifugation in 80 µl adapters in a Fisher model 59 centrifuge at 1500*g* for 5 min. Grids were rinsed with three drops of final dialysis buffer, two drops of stain, and were then stained for 1 min with either 2% uranyl acetate or 2% phosphotungstic acid (PTA) (pH adjusted to 5 with potassium hydroxide). The grids were blotted between each transfer by touching the rim of the grid with filter paper. Uniform staining was only achieved if sucrose and detergent were dialyzed out of the samples. Grids were examined using a Philips EM400T under minimum electron dose conditions (10–20 e Å^{-2}) (Williams & Fisher, 1970). Gap junction plaques were located by scanning the grid at 3600 magnification using a dim beam. Focusing and astigmatism corrections were performed at 170 000 magnification in a field just adjacent to the area to be photographed. Images were recorded on Kodak S0163 film at 46 000 magnification. An optical diffractometer was used to screen different crystallization conditions and select images for data processing that showed the sharpest reflections with uniform staining, minimal astigmatism and minimal drift. Quantitative assessment of astigmatism and drift was provided by radially integrating the Fourier transform in sectors to compare the curvature and minima of the Thon pattern (Thon, 1966) from the carbon film. With this approach the degree of defocus was 5500 to 6500 Å so that the contrast transfer function was uniform and of constant sign to 17 Å resolution (Erickson & Klug, 1971). Micrographs were digitized with a microdensitometer (Perkin-Elmer Corporation, Eden Prairie, MN) using step and aperture sizes of 25 µm.

Image analysis

The extraction and refinement of the crystal lattice parameters and sine-weighted amplitudes was as described (Amos, Henderson & Unwin, 1982). Lattice distortions were corrected using the methods of Henderson, Baldwin, Downing, Lepault & Zemlin (1986). Two-dimensional projection maps were calculated by Fourier transformation using the amplitudes and phases corrected for lattice distortions.

Results

Biochemical characterization

SDS gel electrophoresis profiles (Fig. 2; lane 2) of rat ventricular gap junctions display a primary band corresponding to M_r = 43–45 kDa, close to the value of 43 kDa obtained by molecular cloning (Beyer, Paul & Goodenough, 1987). The Western immunoblot (Fig. 2; lane 3) identifies the 43–45 kDa band as α_1Cx since it is specifically labeled with peptide antibodies directed against amino acids 131–142 in α_1Cx. The profiles indicate that there is minimal proteolysis of α_1Cx.

In situ two-dimensional crystallization by sequential detergent dialysis

The following variables were examined to facilitate crystallization of cardiac gap junctions: detergents (lubrol, octyl-β-D-glucopyranoside, deoxycholate, dodecyl-β-D-maltoside), buffers and solvents (Hepes, Tris, bicarbonate, D_2O), ionic strength (0–150 m*M* NaCl), divalent cations (Ca^{2+} and Mg^{2+}), temperature (heating to 310 K with slow cooling; incubation at 277, 298 and 310 K), and sonication (0–60 s). Smaller cracked sheets are formed if the gap junction suspensions are extensively sonicated. Sonication for 30 s is necessary to break junctional vesicles in order to release trapped soluble contaminants. The sheets

that are formed tend to be more crystalline than vesicular junctions. The critical variables are the choice of detergent and the presence of Mg^{2+}. Best crystals contain areas of 400–600 unit cells and are obtained by sequential dialysis in 0.5% deoxycholate and 0.05% dodecyl-β-D-maltoside as described above (Figs. 3 and 4*a*). Although the gap junctions are crystalline at deoxycholate and dodecyl-β-D-maltoside concentrations over 1%, the sheets show substantial cracking and holes, presumably due to solubilization and formation of protein–detergent micelles. In 5% dodecyl-β-D-maltoside (*i.e.* a detergent concentration 100-fold higher than used in this study), expressed β_1 connexons are completely solubilized as detergent–protein micelles which are amenable to chromatographic purification and crystallization studies (Stauffer, Kumar, Gilula & Unwin, 1991). Higher concentrations of deoxycholate (3–6%) have been used to form two-dimensional crystalline arrays of putative gap junction structures isolated from the lobster hepatopancreas (Sikerwar, Downing & Glaeser, 1991). In addition, protease-treated lens fiber membranes enriched for gap junctions containing cleavage products of α_3Cx can be solubilized in 2–4% octyl-β-D-glucopyranoside (Lampe, Kistler, Hefti, Bond, Müller, Johnson & Engel, 1991).

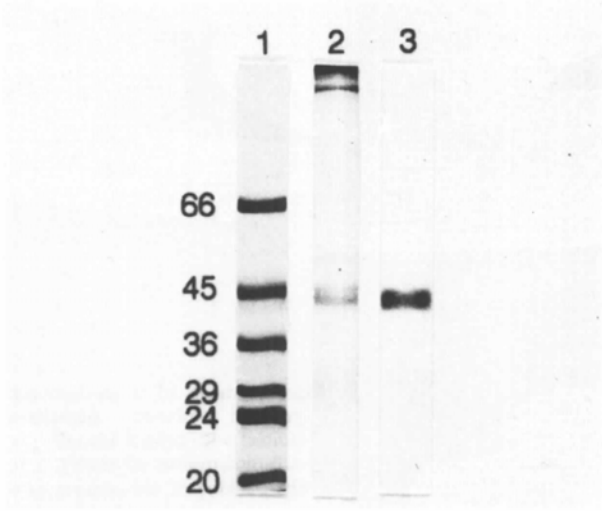

Fig. 2. Cardiac gap junctions isolated using a method similar to that of Manjunath & Page (1986) contain α_1 connexin with M_r = 43 kDa. Coomassie-stained SDS gel electrophoresis profiles of protein molecular weight standards (lane 1) and the 35/49%(*w*/*v*) sucrose density gradient interface containing cardiac gap junctions (lane 2). The Western immunoblot of lane 2 is shown in lane 3 and was generated using affinity-purified peptide antibodies directed against amino acids 131–142 in α_1Cx. The preparations contain native M_r = 43 kDa α_1Cx as well as high-molecular-weight non-connexin insoluble aggregates (see top of lane 2) which are readily distinguished from the gap junction plaques by electron microscopy.

Planar diffraction patterns extend to 16 Å *resolution*

Fig. 4 displays electron micrographs and computer-generated Fourier transforms for cardiac gap junctions negatively stained with uranyl acetate or PTA. The Fourier transforms display hexagonal symmetry, and significant reflections were detectable to 16 Å resolution after lattice straightening. The diffraction patterns derived from junctions stained with uranyl acetate (Fig. 4, left) display weak 1,0 and 0,1 reflections and strong 2,1 and 1,2 reflections. In contrast, the transforms from junctions stained with PTA (Fig. 4, right) display strong 1,0, 0,1; 3,0 and 0,3 reflections, and the 2,1 and 1,2 reflections are weak. These conspicuous differences can be explained by the greater deposition of uranyl stain within the channel compared with PTA. If the crystallization conditions are carried out using higher detergent concentrations, the unit-cell dimensions decrease, and there is greater inequality between the 2,1 and 1,2 reflection intensities. The resultant density maps display skewing of the connexons as has been reported for liver connexons packed into smaller hexagonal lattices (Baker, Caspar, Hollingshead & Goodenough 1983; Gogol & Unwin, 1988).

Density map of planar images reveals a hexameric channel

Since the reflections related by sixfold symmetry displayed a mean phase error that was $<18°$, the crystals have been assigned plane group symmetry *p*6. The projection maps calculated with sixfold symmetry (Fig. 4*c*) clearly delineate the hexameric protein oligomers forming a central ion channel. In uranyl acetate, the prominent negative contours in the central channel are due to heavy deposition of stain (Fig. 4*c*, left). The PTA maps show no negative contours in the channel region, suggesting that this stain is comparatively excluded from the channel (Fig. 4*c*, right). The high contrast in the PTA maps delineates the outer boundary of the protein oligomers which have a diameter of ~65 Å.

Discussion

In situ two-dimensional crystallization of integral membrane proteins

In situ two-dimensional crystallization of cardiac gap junctions containing α_1 connexin (also termed Cx43) was accomplished using a sequential detergent dialysis method. Low concentrations of deoxycholate and dodecyl-β-D-maltoside are used so that the protein is not solubilized in micelles. This approach may provide a simple technique for crystallization of other connexins as well as other membrane proteins,

especially those that are labile when solubilized in detergents. The advantages of this method are that the protein is not removed from its native membrane environment, electron microscopic assay for successful crystallization can be performed on μg quantities of protein, and crystallization takes place in days. The principal disadvantage is that the best resolution attained thus far for cardiac gap junction crystals is ~16 Å. Molecular boundaries and quaternary structure can be examined by electron crystallography, but elements of 2° structure are not visualized.

Hexameric channel design of connexins

The Fourier reconstructed two-dimensional density maps (Fig. 4*c*) reveal that the α_1Cx molecules are arranged as hexameric clusters with a diameter of ~65 Å. Differential staining by uranyl acetate and phosphotungstic acid provides further definition of the α_1 connexon. Uranyl acetate penetrates the channels (Fig. 4*c*, left) much more readily that PTA (Fig. 4*c*, right). PTA is preferentially deposited over the membrane regions and delineates the boundary between the connexons and the lipid regions. This differential staining is comparable to that observed with liver gap junctions (Baker, Sosinsky, Casper, Gall & Goodenough, 1985) and may be particularly useful to characterize the conformational changes associated with channel gating in different physiologic states, as may occur with changes in Ca^{2+} or pH (Ramón & Rivera, 1986; Spray & Burt, 1990). The hexameric structure of cardiac gap junction ion channels formed by α_1Cx is comparable to that of mouse liver junctions containing β_1Cx and β_2Cx, rat liver junctions primarily formed by β_1Cx, and protease-cleaved α_3Cx in lens gap junctions. The hexameric design of gap junctions therefore appears to be a recurring quaternary motif for the multigene family of gap junction proteins.

I gratefully acknowledge the encouragement of Nigel Unwin and computer programs provided by Richard Henderson, Nigel Unwin, Chikashi Toyoshima and Ed Gogol. This work has been supported by the NIH, the American Heart Association, National Center (Grant-in-Aid 90228120) and the Gustavus and Louise Pfeiffer Research Foundation. MY is an Established Investigator of the American Heart Association and Bristol-Myers Squibb.

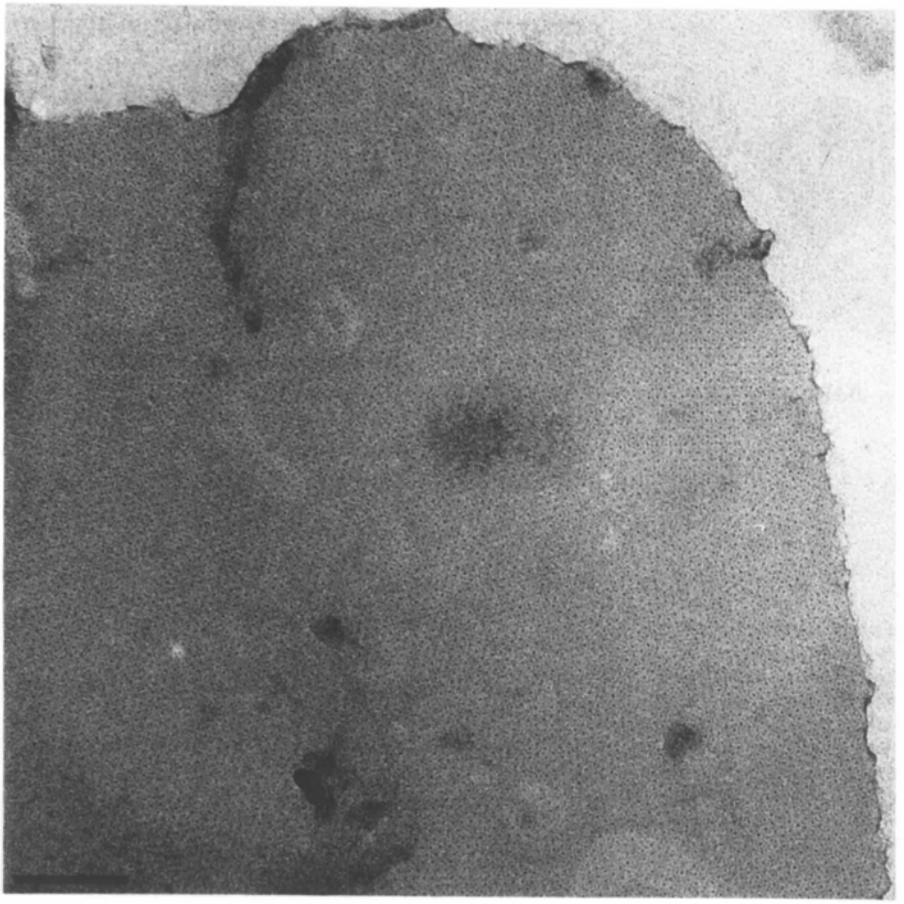

Fig. 3. Image of a cardiac gap junction plaque negatively stained with uranyl acetate. The two-dimensional crystallinity in the packing of the connexons is a consequence of detergent treatment with deoxycholate and dodecyl-β-D-maltoside. The plaque displays a mosaic of crystalline domains, the largest of which is ~0.5 μm^2. This gap junction preparation has undergone protease cleavage (see arrow in Fig. 1) which presumably accounts for the increased clarity of the connexons in this image compared with Fig. 4(*a*). Scale bar 1000 Å.

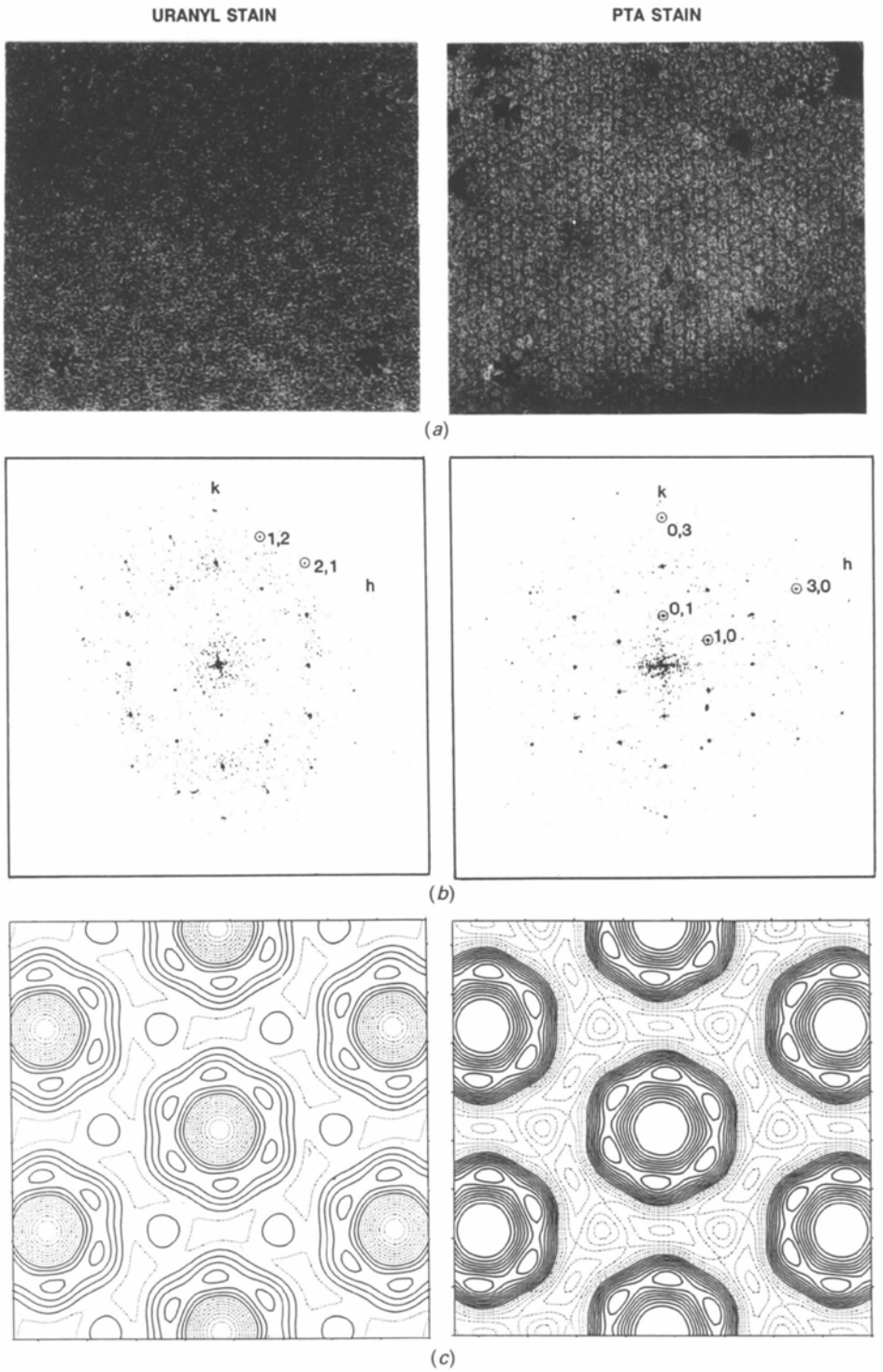

Fig. 4. Images (*a*) of cardiac gap junctions stained with either 2% uranyl acetate (left) or 2% phosphotungstic acid (right). The asterisks (*) define the boxed areas judged most crystalline by optical diffraction. The arms of the asterisks are roughly aligned with the axes of the hexagonal crystals. The computed diffraction patterns (*b*) have hexagonal symmetry, and the digitized patterns extend to 16 Å resolution. Two-dimensional projection maps were calculated by Fourier transformation (*c*). The ion channels are formed by hexameric clusters of protein subunits (continuous, positive contours). Uranyl acetate enters the central channel (circular dashed contours), whereas phosphotungstic acid preferentially binds to membrane lipids to define the boundary between the protein subunits and the lipid bilayer regions. Scale marks are 20 Å, and the center-to-center separation between the hexameric oligomers is 85 Å. Adapted from Yeager & Gilula (1992).

References

Amos, L. A., Henderson, R. & Unwin, P. N. T. (1982). *Prog. Biophys. Mol. Biol.* **39**, 183–231.

Baker, T. S., Caspar, D. L. D., Hollingshead, C. J. & Goodenough, D. A. (1983). *J. Cell Biol.* **96**, 204–216.

Baker, T. S., Sosinsky, G. E., Casper, D. L. D., Gall, C. & Goodenough, D. A. (1985). *J. Mol. Biol.* **184**, 81–98. (Also see other references in this series.)

Barr, L., Dewey, M. M. & Berger, W. (1965). *J. Gen. Physiol.* **48**, 797–823.

Beyer, E. C., Kistler, J., Paul, D. L. & Goodenough, D. A. (1989). *J. Cell Biol.* **108**, 595–605.

Beyer, E. C., Paul, D. L. & Goodenough, D. A. (1987). *J. Cell Biol.* **105**, 2621–2629.

Beyer, E. C., Paul, D. L. & Goodenough, D. A. (1990). *J. Membr. Biol.* **116**, 187–194.

Caspar, D. L. D., Goodenough, D. A., Makowski, L. & Phillips, W. C. (1977). *J. Cell Biol.* **74**, 605–628.

Erickson, H. P. & Klug, A. (1971). *Philos. Trans. R. Soc. London Ser. B*, **261**, 105–118.

Gogol, E. & Unwin, N. (1988). *Biophys. J.* **54**, 105–112.

Henderson, R., Baldwin, J. M., Downing, K. H., Lepault, J. & Zemlin, F. (1986). *Ultramicroscopy*, **19**, 147–178.

Jap, B. K., Zulauf, M., Scheybani, T., Hefti, A., Baumeister, W., Aebi, U. & Engel, A. (1992). *Ultramicroscopy*, **46**, 45–84.

Kühlbrandt, W. (1992). *Q. Rev. Biophys.* **25**, 1–49.

Kumar, N. M. & Gilula, N. B. (1992). *Semin. Cell Biol.* **3**, 3–16.

Laemmli, U. K. (1970). *Nature (London)*, **227**, 680–685.

Laird, D. W. & Revel, J.-P. (1990). *J. Cell Sci.* **97**, 109–117.

Lampe, P. D., Kistler, J., Hefti, A., Bond, J., Müller, S., Johnson, R. G. & Engel, A. (1991). *J. Struct. Biol.* **107**, 281–290.

Loewenstein, W. R. (1981). *Physiol. Rev.* **61**, 829–913.

Makowski, L., Caspar, D. L. D., Phillips, W. C. & Goodenough, D. A. (1977). *J. Cell Biol.* **74**, 629–645.

Manjunath, C. K., Goings, G. E. & Page, E. (1985). *J. Membr. Biol.* **85**, 159–168.

Manjunath, C. K., Nicholson, B. J., Teplow, D., Hood, L., Page, E. & Revel, J.-P. (1987). *Biochem. Biophys. Res. Commun.* **142**, 228–234.

Manjunath, C. K. & Page, E. (1986). *J. Membr. Biol.* **90**, 43–57.

Ramón, F. & Rivera, A. (1986). *Prog. Biophys. Mol. Biol.* **48**, 127–153.

Spray, D. C. & Burt, J. M. (1990). *Am. J. Physiol.* **258**, C195 205.

Sikerwar, S. S., Downing, K. H. & Glaeser, R. M. (1991). *J. Struct. Biol.* **106**, 255–263.

Sikerwar, S. S. & Unwin, N. (1988). *Biophys. J.* **54**, 113–119.

Stauffer, K. A., Kumar, N. M., Gilula, N. B. & Unwin, N. (1991). *J. Cell Biol.* **115**, 141–150.

Thon, F. (1966). *Z. Naturforsch. Teil a*, **21**, 476–478.

Towbin, H., Staehelin, T. & Gordon, J. (1979). *Proc. Natl Acad. Sci. USA*, **76**, 4350–4354.

Unwin, P. N. T. & Ennis, P. D. (1984). *Nature (London)*, **307**, 609–613.

Unwin, P. N. T. & Zampighi, G. (1980). *Nature (London)*, **283**, 545–549.

Willecke, K., Hennemann, H., Dahl, E., Jungbluth, S. & Heynkes, R. (1991). *Eur. J. Cell Biol.* **56**, 1–7.

Williams, R. C. & Fisher, H. W. (1970). *J. Mol. Biol.* **52**, 121–123.

Yancey, S. B., John, S. A., Lal, R., Austin, B. J. & Revel, J.-P. (1989). *J. Cell Biol.* **108**, 2241–2254.

Yeager, M. & Gilula, N. B. (1992). *J. Mol. Biol.* **223**, 929–948.